Connection between the flickering and the mass outflow in the symbiotic binary star MWC 560

R. K. Zamanov[1], T. Tomov[2], M. F. Bode[3], M. Mikołajewski[2],
K. A. Stoyanov[1], V. Stanishev[4]

[1] Institute of Astronomy and NAO, Bulgarian Academy of Sciences, 1784 Sofia, Bulgaria
[2] Centre for Astronomy, Nicolaus Copernicus University, 87-100 Toruń, Poland
[3] Astrophysics Research Institute, Liverpool John Moores University, CH41 1LD, UK
[4] CENTRA - Centro Multidisciplinar de Astrofísica, Instituto Superior Técnico, 1049-001 Lisbon, Portugal
rkz@astro.bas.bg

(Research report. Accepted on 02.11.2010)

Abstract. We analyze archival U-band high speed photometry of the jet-ejecting symbiotic binary MWC 560 obtained during 1990–1993. The analysis shows that variability on time scales <20 min (flickering) is missing when the mass outflow is in a regime of discrete ejections with ejection velocity V_{ej} up to 7000 $\mathrm{km\,s^{-1}}$(February 1990 – March 1991), and when the outflow has stable low velocity ∼900 $\mathrm{km\,s^{-1}}$ (October 1990 – March 1991). Short term variability on time scales of 10–15 minutes is present when the outflow has a stable velocity ∼2000 $\mathrm{km\,s^{-1}}$ (December 1991 – January 1993). The flickering amplitude is also influenced by the different states of the jet. A comparison with T CrB shows also that the variability of MWC 560 on time scales $\leq 5-10$ min is considerably lower. Supposing that the flickering originates in an accretion disk it means that the observed phenomenon is similar to the disk-jet connection in CH Cyg (Sokoloski & Kenyon 2003a). The probable interpretation is that the accretion disk (flow) in MWC 560 is able to switch between different states like in the galactic microquasars.

Key words: stars: individual: MWC 560 – binaries: symbiotic – binaries:novae, cataclysmic variables

Връзка между фликеринга и загубата на маса при симбиотичната двойна звезда MWC 560

Р.К.Заманов, Т. Томов, М.Ф. Боде, М. Миколайевски, К.А. Стоянов, В. Станишев

В тази статия изследваме фотометричните наблюдения в U-филтър на симбиотичната звезда MWC 560 за периода 1990-1993 г. Анализът показва, че няма периодичност за времеви скали < 20 мин (фликеринг), когато материята се изхвърля със скорости V_{ej} до 7000 $\mathrm{km\,s^{-1}}$(февруари 1990 – март 1991) и когато потокът от изхвърлена материя има постоянна малка скорост ∼ 900 $\mathrm{km\,s^{-1}}$(октомври 1990 – Март 1991). Наблюдава се късопериодична променливост за времева скала от 10–15 мин, когато потока е с постоянна скорост ∼ 2000 $\mathrm{km\,s^{-1}}$(декември 1991 – януари 1993). Амплитудата на фликеринга също зависи и от различните състояния на джета. Сравнението с T CrB показват, че променливостта на MWC 560 за времеви скали $\leq 5-10$ мин е значително по-малка. Предполагайки, че източникът на фликеринг е акреционният диск, можем да заключим, че наблюдаваното явление е подобно на наблюдаваната връзка диск-джет при CH Cyg (Sokoloski & Kenyon 2003a). Вероятното заключение е, че акреционния диск (поток) на MWC 560 може да включва различни състояния подобно на микроквазарите.

Introduction

The widely accepted model of MWC 560 (V694 Mon, LS 391) is that it is a binary system consisting of a red giant and a white dwarf (most probably magnetic). The binary period is about 1931 days (Gromadzki et al. 2007) and the orbit is highly eccentric ($e \sim 0.7$, Zamanov et al. 2010). The system is visible almost face-on. The most spectacular phenomenon associated with this object is the collimated outflow (jet), whose axis coincides approximately with the line of sight. The velocity of the outflow varies from a few hundred km s^{-1} to 7000 km s^{-1} (i.e. Tomov et al, 1990; Schmid et al. 2001). The object also shows short term variability (flickering).

The flickering (stochastic brightness variations), occurring on time scales of minutes with amplitudes ranging from a few millimagnitudes up to more than one magnitude is a phenomenon typical for cataclysmic variables, and it is rarely observed in symbiotic stars. For example, to-date it is detected in only 9 (including MWC 560) of the 220 known symbiotics (Dobrzycka et al. 1996; Belczyński et al. 2000, Sokoloski, Bildsten & Ho 2001). The exact origin of the flickering is not clear, but it is considered to be a result of accretion onto the white dwarf (WD) through a disk. The possible mechanisms include unstable mass transfer, magnetic discharges, turbulence and instability in the boundary layer (e.g. Warner 1995, Bruch 1992).

A disk-jets connection has been discovered and analyzed in galactic microquasars and X-ray binaries, i.e. Cygnus X-1 (Brocksopp et al. 1999), GX 339-4 (Corbel et al. 2000), GRS 1915+105 (Belloni et al. 2000), Cygnus X-3 (Choudhury et al. 2002). Similar mechanisms probably operate at accretion onto suppermassive black holes in active galactic nuclei (*e.g.* Mirabel & Rodriguez 1998). A disk-jet connection was postulated for the 1997 jet launch from the WD in CH Cyg by Sokoloski & Kenyon (2003a,b), who have interpreted the prominent minimum in the light curve as the inner disc disruption, associated with the mass ejection event. It is important to note that such behaviour is closely analogous to that of the black hole accretors as galactic microquasar GRS 1915+105 and AGNs (Livio, Pringle & King 2003). The knowledge of a disk-jet connection in different accreting sources will help us to understand a Mario Livio's idea: is there a common, accretion-powered mechanism for formation of all jets (*e.g.* Livio 1997, 1998)?

Here we analyze the high-speed flickering observations of MWC 560 with the aim of seing if there is a difference between the flickering properties when the star is in different regimes of mass outflow, supposing that the flickering originates in an accretion disk around the white dwarf.

1 Data

The data used here are described and analyzed for the presence of quasi-periodic oscillations in Tomov et al. (1996). The advantage of this data set is that there are spectra obtained in the same seasons from January 1990 untill March 1993 (Tomov & Kolev 1997). The star is observable from October till April and the spectra as well as the photometry are obtained in the same annual intervals. This permits us to investigate the connection between the different mass ejection regimes (described above) and the flickering properties of the system, in other words the disk-jet connection. From the high-speed photometry of Tomov et al. (1996) we selected only the U band observations because (1) they are majority; (2) the flickering amplitude is usually biggest in U band; (3) the red giant contribution in U is small. A journal of

the observations, together with measured parameters (see Sect.3), is given in Table 1.

2 Mass outflow regimes

The mass outflow of MWC 560 has the form of collimated jets (Tomov et al. 1992, Shore, Aufdenberg & Michalitsianos, 1994). There are different states of the mass outflow which are reflected in the shape of the absorption component of Balmer lines. For example, Iijima (2002) has classified them into four types, dependent on steepness or slope shape on both sides of the absorption and the existence (or not) of a flat continuum between emission and absorption components.

Taking into account the shape of the absorption components, values of their velocities and time-scale of their evolution observed during the time of our high speed photometry we can distinguish three periods characterized by three different regimes of mass outflow (Tomov & Kolev 1997):

(i) January 1990 - April 1990 – *discrete ejections* with extremally high velocities V_{ej} up to 7000 km s^{-1}, which appear and disappear on a time scale of 1-2 days. There are also observations when the high velocity absorption components are not visible.

(ii) December 1990 - March 1991 – *stationary outflow* with velocity $\sim$900 km s^{-1}, measured at the blue edge of the absorption lines.

(iii) September 1991 - March 1993 – *stationary outflow* with V_{ej} $\approx$2000 km s^{-1}.

During the time intervals January 1990 - April 1990 and September 1991 - March 1993 the absorption component is separated from the emission by a section of flat continuum (C and D type in Ijima's classification). The profiles are not similar to the classical P Cygni type. During December 1990 - March 1991 the profiles look like classical P Cygni profiles (A-type in Ijima's classification), however this can be a result of the lower velocity of mass ejection.

An inspection by eye of our data has shown that the flickering properties during the described periods with different regimes of the mass outflow are also different (dates in format [yymmdd]):

(i) 900224 – 900402 - smooth light curves with typical time scale about $\geq$1 hour.

(ii) 901028 – 910323 - smooth light curves, similar to those observed during the previous period **(i)**, sometimes with almost no variability. The typical time scale is difficult to be defined.

(iii) 911213 – 930123 - larger amplitude variations on timescales from 10 min to $\sim$1 hour. Identical variability is also visible in the data of Michalitsianos et al.(1993) obtained on 26/02/1992, 03/03/1992 and 10/10/1992.

In the next section we try to find some objective, mathematical parameters and representations which can confirm this.

3 Flickering quantities

The measured parameters are summarized in Table 1 (in a manner similar to Zamanov et al. 2004). The standard deviation, and autocorrelation function have been defined **both, before and after** a tension spline subtraction. The tension spline interpolation fit is done through the mean points in non-overlapping bins of length

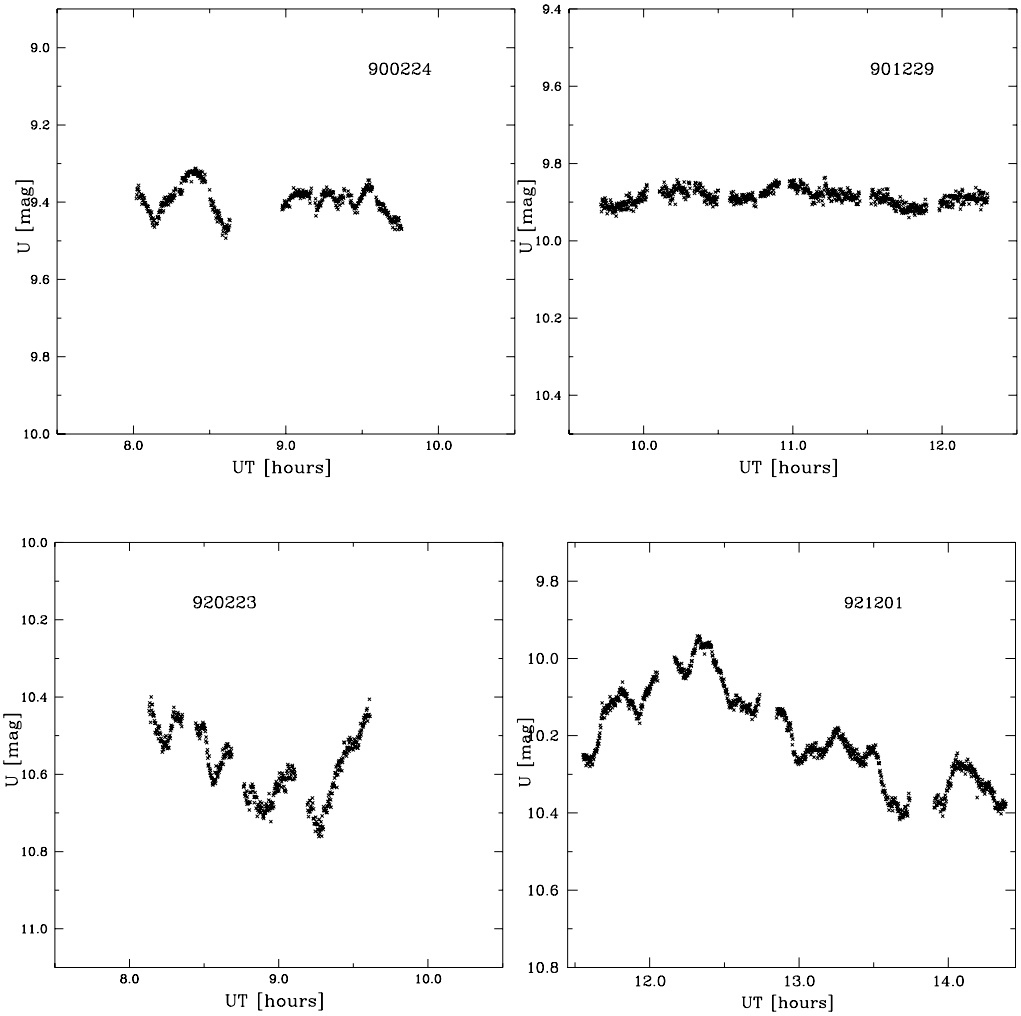

Fig. 1. Examples of the flickering behaviour of MWC 560. Date is in the format YYMMDD.

$\sim$20 minutes in a way that is identical to that applied to TT Ari by Kraicheva et al. (1999) and T CrB (Zamanov et al. 2004). In this way we remove the variability on $\sim$1 hour time scales and are able to define some of the properties on longer time scales (before the spline) and on shorter time scales (after the spline interpolation).

3.1 The standard deviation

To demonstrate that the visual impression is a real fact, we calculated the standard deviation for the original light curves (σ_0) and after the subtraction of a spline fit (σ_1). The values σ_1 versus σ_0 are plotted on Fig.2. The standard deviation (for all 33 runs) takes values $\sigma_0 = 0.02 - 0.21$, with $\overline{\sigma}_0 = 0.08 \pm 0.04$ and $\sigma_1 = 0.01 - 0.06$, $\overline{\sigma}_1 = 0.03 \pm 0.01$, where all values are in magnitudes.

As is visible in Fig.2 the open symbols covering periods (i) and (ii) occupy the left low corner and filled symbols (period iii) are located above them. This indicates the presence of larger variability on shorter time scales during 911213 – 930123. For the period 900224 – 910323 (18 runs) we calculate $\sigma_0 = 0.02 - 0.11$, $\overline{\sigma}_0 = 0.05 \pm 0.03$ and $\sigma_1 = 0.009 - 0.035$, $\overline{\sigma}_1 = 0.020 \pm 0.008$. For the period 911213 – 940114 (14 runs) $\sigma_0 = 0.055 - 0.212$, $\overline{\sigma}_0 = 0.11 \pm 0.04$ and $\sigma_1 = 0.031 - 0.054$, $\overline{\sigma}_1 = 0.043 \pm 0.008$.

Similar analysis of the flickering in the well known recurrent nova T CrB was done by Zamanov & Bruch (1998) and Zamanov et al. (2004). The standard deviation takes values $\sigma_0 = 0.04 - 0.12$, $\overline{\sigma}_0 = 0.08 \pm 0.02$ and $\sigma_1 = 0.04 - 0.09$, $\overline{\sigma}_0 = 0.06 \pm 0.02$. A comparison with T CrB shows that the variability of MWC 560 on longer time scales ($\sim$1 hour) can be lower, similar or greater than T CrB (see σ_0). However, on shorter time scales ($\leq$15 min), the variability of MWC 560 is (almost) always lower than that of T CrB (see the values of σ_1).

3.2 Power spectra

For each run we also calculated the power spectrum. The power spectra of MWC 560 light curves follow approximately a power law $P(f) \propto f^{\gamma}$, where P is the power and f is the frequency. The power-law index γ was determined in the frequency interval from 3 to 160 cycles/hour. In practice, we fitted the power spectra over this interval in log-log scale with a linear least-squares fit: $\log(P) = A + \gamma \log(f)$. γ and A are given in Table 1. The typical errors are ΔA= ± 0.8 and $\Delta\gamma = \pm 0.25$.

The power-law index takes values in the range γ = -1.74 – -0.58, $\overline{\gamma} = -0.96 \pm 0.23$. This makes the power spectra law different from that observed in T CrB $\overline{\gamma} = -1.46 \pm 0.17$. A Kolmogorov-Smirnov test that both distributions of γ are from the same parent population gives probability $\sim 10^{-9}$. Our experiments have shown that this difference is mainly due to the lack of large amplitude variations on time scales of ≤ 5 min in MWC 560 and their presence in T CrB, which is also visible in the calculated standard deviation and auto-correlation function.

The power-law spectrum of the type observed in T CrB is expected in the model of flickering proposed by Yonehara, Mineshige & Welsh (1997). They proposed as the origin of flickering a self-organised critical state of the disk in which seemingly chaotic fluctuations can be produced. Such a model implies $\gamma \simeq -(1 - 2)$. Our observations of MWC 560 do not contradict this model.

Table 1. Journal of flickering observations of MWC 560 in the Johnson U band. Date is given in the format YYMMDD, N is the number of the points in the run, D is the duration of the run in minutes. U_{max}, U_{min}, and U_{aver} are the maximum brightness during the night, the minimum, and the average of this quantity, respectively. The standard deviation is given for the original run (σ_0), and after subtraction of a spline fit (σ_1). U_{av} is calculated averaging the corresponding fluxes. The power spectra in each night are fitted with a linear fit (A and γ are the parameters of the fit). γ is the power spectrum slope in the interval 3-160 cycles/hour. The e-folding time of the ACF is given for the original run (τ_0), and after subtraction of a spline fit (τ_1).

Date	N	D [min]	U_{max} [mag]	U_{min} [mag]	U_{av} [mag]	σ_0 [mag]	σ_1 [mag]	A	γ	τ_0 [sec]	τ_1 [sec]
900224	455	104	9.312	9.493	9.395	0.037	0.034	-0.712	-1.317	267 ±18	251±20
900225	863	222	9.440	9.867	9.613	0.108	0.019	-1.523	-0.838	3124 ±349	110±12
900226	864	222	9.429	9.823	9.645	0.096	0.027	-1.204	-0.969	1725 ±35	143±25
900305	350	85	9.415	9.596	9.499	0.048	0.026	-1.034	-0.925	413 ±35	203±13
900306	408	83	9.351	9.549	9.441	0.043	0.021	-1.105	-0.891	988 ±42	77±30
900306	424	102	9.333	9.498	9.413	0.039	0.014	-0.877	-1.018	562 ±26	83±56
900314	282	59	9.530	9.651	9.590	0.026	0.018	-0.618	-1.066	246 ±20	201±24
900401	224	45	9.065	9.229	9.151	0.032	0.029	-0.597	-1.077	125 ±16	123±20
900402	286	65	8.960	9.204	9.084	0.064	0.014	-0.709	-1.083	792 ±33	123±24
901026	148	33	9.922	10.007	9.960	0.019	0.009	-0.629	-0.813	511 ±27	38±0
901221	498	105	9.880	10.326	10.149	0.102	0.021	-0.946	-0.918	1258 ±22	230±36
901224	552	115	9.778	10.143	9.940	0.093	0.018	-1.499	-0.772	1764 ±36	125±37
901229	849	186	9.807	9.939	9.883	0.024	0.012	-1.627	-0.810	592 ±34	25±17
901230	496	104	9.761	10.099	9.962	0.068	0.035	-1.422	-0.717	542 ±92	99±25
901230	482	99	9.867	9.969	9.915	0.019	0.013	-1.215	-0.853	708 ±64	62±7
910104	865	261	9.668	9.881	9.782	0.045	0.017	-1.164	-1.006	686 ±18	207±16
910121	794	221	9.606	9.876	9.710	0.068	0.013	-1.201	-0.954	2079 ±58	93±37
910323	320	104	9.798	9.944	9.875	0.031	0.014	0.326	-1.745	702 ±40	76±28
911213	858	174	10.122	10.514	10.305	0.086	0.037	-1.476	-0.872	1611 ±44	190±11
911215	372	90	10.346	10.652	10.533	0.084	0.039	-0.658	-0.975	758 ±32	172±9
911216	864	170	9.997	10.528	10.225	0.106	0.054	-1.444	-0.829	707 ±66	218±13
920223	447	88	10.399	10.761	10.579	0.088	0.042	-1.201	-0.840	609 ±30	183±11
921124	848	200	10.060	10.551	10.307	0.100	0.051	-1.197	-0.924	759 ±61	297±26
921201	883	169	9.942	10.417	10.200	0.120	0.031	-2.101	-0.669	2332 ±57	195±9
921202	557	105	9.682	10.328	9.938	0.212	0.032	-1.852	-0.671	1258 ±90	230±17
921203	567	105	10.196	10.529	10.348	0.084	0.032	-1.921	-0.580	1233 ±33	225±13
921205	314	60	9.818	10.361	10.085	0.170	0.054	-0.604	-1.047	786 ±31	297±23
921229	1191	276	10.501	10.958	10.714	0.095	0.048	-2.082	-0.669	2160 ±123	220±15
930118	280	220	10.519	10.813	10.672	0.055	0.050	-0.977	-0.987	173 ±53	159±16
930119	440	268	10.567	11.085	10.822	0.109	0.045	-0.952	-1.052	580 ±471	162±12
930121	220	133	10.624	11.128	10.857	0.122	0.048	-0.687	-1.113	458 ±98	161±35
930123	476	307	10.584	11.217	10.887	0.136	0.036	-0.707	-1.279	1355 ±307	59±20

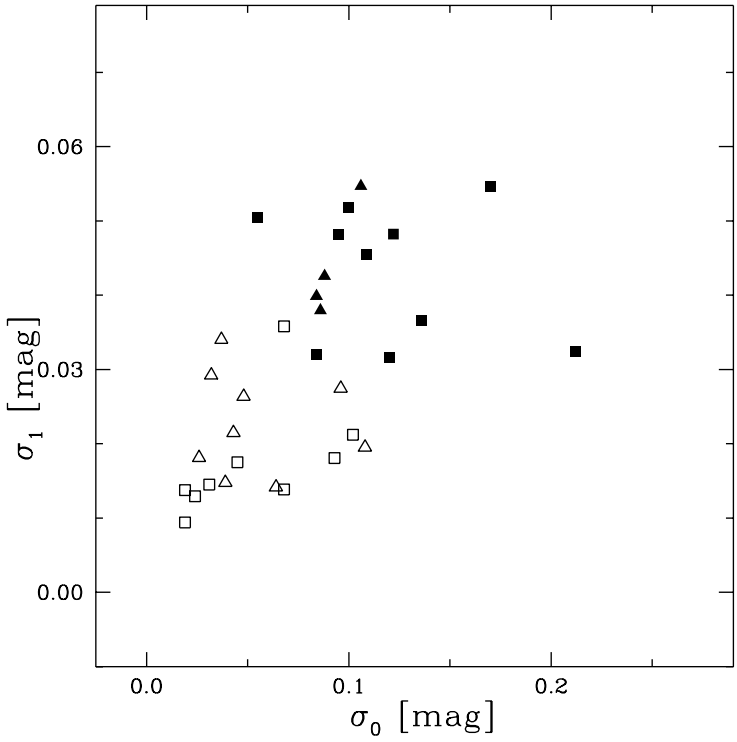

Fig. 2. The standard deviation σ_1(after subtraction of a spline fit) versus σ_0 (for the original run). The symbols refer as follows:
from 900225 to 900402 – open triangles
from 901026 to 910323 – open squares,
from 911213 to 920223 – solid triangles,
from 921124 to 930123 – solid squares.
The solid triangles and the solid squares occupy the same place on all figures in agreement with the fact that the mass outflow visible in the spectra is identical during these two seasons.

3.3 Autocorrelation function (ACF)

Another objective way to investigate flickering behaviour (see also Bruch 2000) is the autocorrelation function (ACF). The ACFs is calculated according to Edelson & Krolik (1988) for unevenly spaced data.

The e-folding time of the ACF (which is a representation of the typical time scale of the variability) is defined as the time shift at which the ACF first reaches the value $1/e$. Thus determined correlation times are influenced by the presence of periodic brightness variations, trends in the data, the presence of weakly correlated noise, and the process of trend removal [see also Robinson & Nather (1971) and Panek (1980)].

The e-folding time is given in Table 2. The errors are determined from the errors of the autocorrelation coefficients. We calculated e-folding times in two different ways: (i) the e-folding time of the ACF of the original data in each run (τ_0) and (ii) after subtraction of a spline fit (τ_1), as described in Sect.1. Operation (ii) has been done in order to obtain the e-folding time on shorter time scales.

In Fig.3 are shown τ_1 versus τ_0 for MWC 560 (left panel) and T CrB (right panel). It is apparent that the scatter of the points for MWC 560 is considerably bigger than for T CrB. It indicates that the variability of MWC 560 has considerably longer typical time scale than of T CrB.

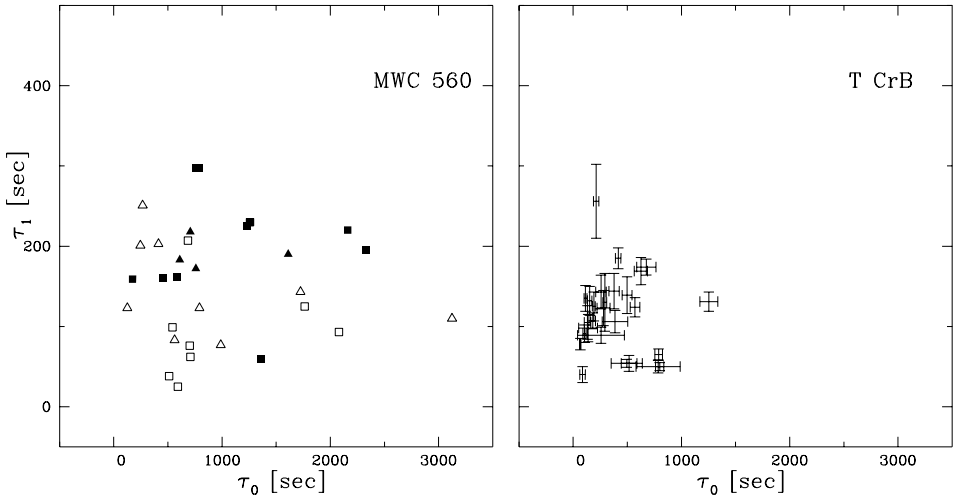

Fig. 3. e-folding time of the ACF for MWC 560 (left panel) and T CrB (right panel). X-axis (τ_0) is before subtraction of a spline, Y-axis (τ_1) is after subtraction of a spline. It is obvious that the scatter of the points for MWC 560 is considerably bigger than that of T CrB. The symbols on the left panel are the same as in Fig.2. On the right panel the data points are plotted with the corresponding errors.

3.4 The full flickering amplitude

Before defining the average flux of the hot component we need to subtract the red giant contribution. For MWC 560 the minimum brightness in Johnson V band observed untill now is V=10.2 (Tomov et al. 1996) and the red giant is classified as M5.5 III (Schmid et al. 2001). Using (U-V)$_{M5.5III}$=2.80 - 2.95 (Lee, 1980; Schmidt-Kaler 1982; Fluks 1994), and the reddening $E_{\rm U-V} \approx 0.3$ we adopt the contribution of the red giant equivalent to U≈ 13.3.

Thus the full flickering amplitude ΔF and average flux of the hot component $F_{\rm av}$ were derived from corresponding values $U_{\rm max}$, $U_{\rm min}$ and $U_{\rm av}$ (Table 1) and using the value 4.194×10^{-11} Wm^{-2}nm^{-1} as the zero U magnitude flux (Bessel 1979).

The flickering amplitude ΔF versus the average flux of the hot component $F_{\rm av}$ is plotted in Fig.4. Both, ΔF and $F_{\rm av}$ have a range of about one order of magnitude, very similar to T CrB, whereas the same ranges for CH Cyg are about two orders of magnitude (see Fig. 6 in Zamanov et al. 2004). Nevertheless, only T CrB shows one population of points on the ΔF – $F_{\rm av}$ diagram, when both CH Cyg and MWC 560 probably display two populations of points with flickering proportional to averaged flux, along two shifted lines (see also Mikolajewski et al. 1990).

In Fig.4 the correlations between ΔF and $F_{\rm av}$ for different regimes of the outflow are visible. The scatter of the points is bigger during the period of the first and second observational season (900224 – 910323), however the points from the second season (open squares in Fig.4) seem to connect points of both populations at roughly constant average flux. During 911213 – 930123 it seems to follow a tight relation. This indicates that total amplitude of the variability (in 1-2 hours runs) is also connected with the mass outflow. The relationship of ΔF with the average and/or the minimum flux can be connected with the magnetic field of the WD (Zamanov et al. 2004) or with the size of the boundary layer between the WD and the accretion disk (Bruch & Duschl 1993). How this correlation works in the case when the inner disk is disrupted by the outflow is unclear.

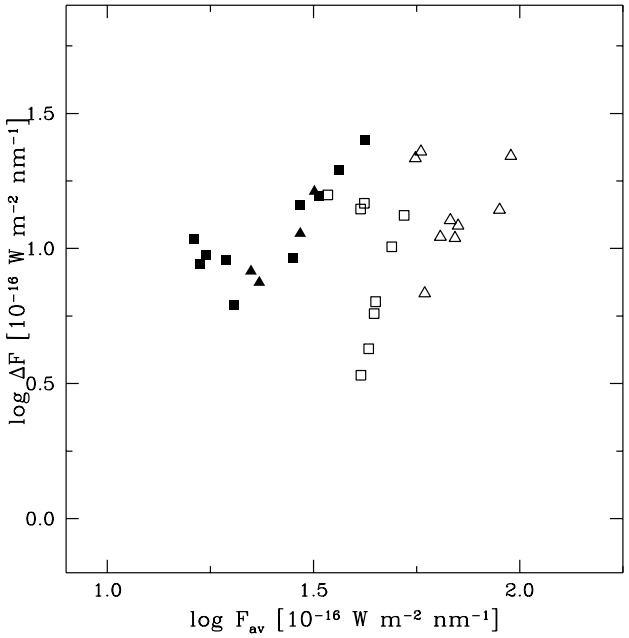

Fig. 4. The flickering amplitude versus the flux of the hot component in the U band for MWC 560. The axes are in units of 10^{-16} Watt $\rm m^{-2}nm^{-1}$. The contribution of the red giant has been removed. The symbols on the left panel are the same as in Fig.2.

4 Discussion

4.1 Velocity of the outflow

Let us suppose that the outflow velocity V_{ej} corresponds to the escape velocity at the place where the outflow originates. This is a general picture for almost all jets (Livio 1997, 1998). Using

$$V_{ej} \sim V_{esc} = \sqrt{2GM_{wd}/R_{ej}}, \quad (1)$$

where G is the gravitational constant, M_{wd} is the WD mass. R_{ej} is the distance from the accreting object where the outflow originates. The observed ejection velocities of about 6000-7000 km s^{-1} correspond to an escape velocity close to the surface of the WD. If this is the escape velocity on the surface of the WD following the mass-radius relation for magnetic or non-magnetic WDs (e.g. Suh & Mathews 2000, Madej, Należyty & Althaus 2004) this will infer a rather small and massive object: $R_{wd} \approx 4 \times 10^8$ cm and $M_{wd} \approx$1.2 $M_\odot$.

If this is strictly correct the origin of the outflow is at
(i) $R_{ej} \approx 1\ R_{wd} = 0.006\ R_\odot$ for $V_{ej} \approx 6000$ km s^{-1},
(ii) $R_{ej} \approx$50 $R_{wd} = 0.25\ R_\odot$ for $V_{ej} \approx 900$ km s^{-1}, and
(iii) $R_{ej} \approx$10 $R_{wd} = 0.06\ R_\odot$ for $V_{ej} \approx 2000$ km s^{-1},
for three regimes defined in Sect.2, respectively.

4.2 Flickering time scales

A useful tool for defining the time scales of the flickering is the ACF. The examples shown by Robinson and Nather (1979) and Bruch (2000) demonstrate that the e-folding time is a good representation of the typical time scale of the variability. In Fig.5 are displayed the values of time scales τ_0 and τ_1 against to $U_{\rm av}$ magnitude. For four shortest e-folding times $\tau_0 \approx \tau_1$ (see Table 1) i.e. the ACF does not detect the long time scale variability. Most of other values of τ_0 form the pronounced, sharp peak between 400 and 800 sec with the mean value $\overline{\tau}_0 = 697 \pm 38$ sec for 16 runs $\overline{\tau}_0 = 678 \pm 34$ sec for 15 runs. We will define this timescale as the 11.5 ± 0.6 min variability. About a dozen values of τ_0 for other runs form a broad long tail with timescales between 17 and 50 minutes. Both, points belonging to 11.5 min peak and to broad tail of τ_0 have no correlation with luminosity or mass outflow regime (Fig. 5).

Another situation concerns the shorter τ_1 timescales which form two populations of points similar to that observed for the flickering amplitude (Fig. 4). Both populations seem to slightly lengthen the timescale τ_1 with luminosity showing a sharp jump of this timescale from about 30-120 sec for $U_{\rm av} \leq 10.0$ mag to about 200-300 sec for $U_{\rm av} \geq 10.0$ mag. The same discontinuity around $U_{\rm av} \approx 10.0$ is also visible in Fig. 6 for values of standard deviations σ_0 and most significantly for σ_1. Variations of σ_0 in upper panel of Fig. 6 are practically the same as the flickering amplitude in Fig. 4 assuming $\Delta F \approx F(U_{av} - 3\sigma_0) - F(U_{av} + 3\sigma_0)$. The change of standard deviation σ_0 around 10th magnitude can reach even one order of magnitude. Standard deviation $\overline{\sigma}_1 \approx 0.04 \pm 0.01$ seems to be almost constant for $U_{\rm av} \gtrsim 10.0$ mag. Also for $U_{\rm av} \lesssim 10.0$, there seems to be almost constant

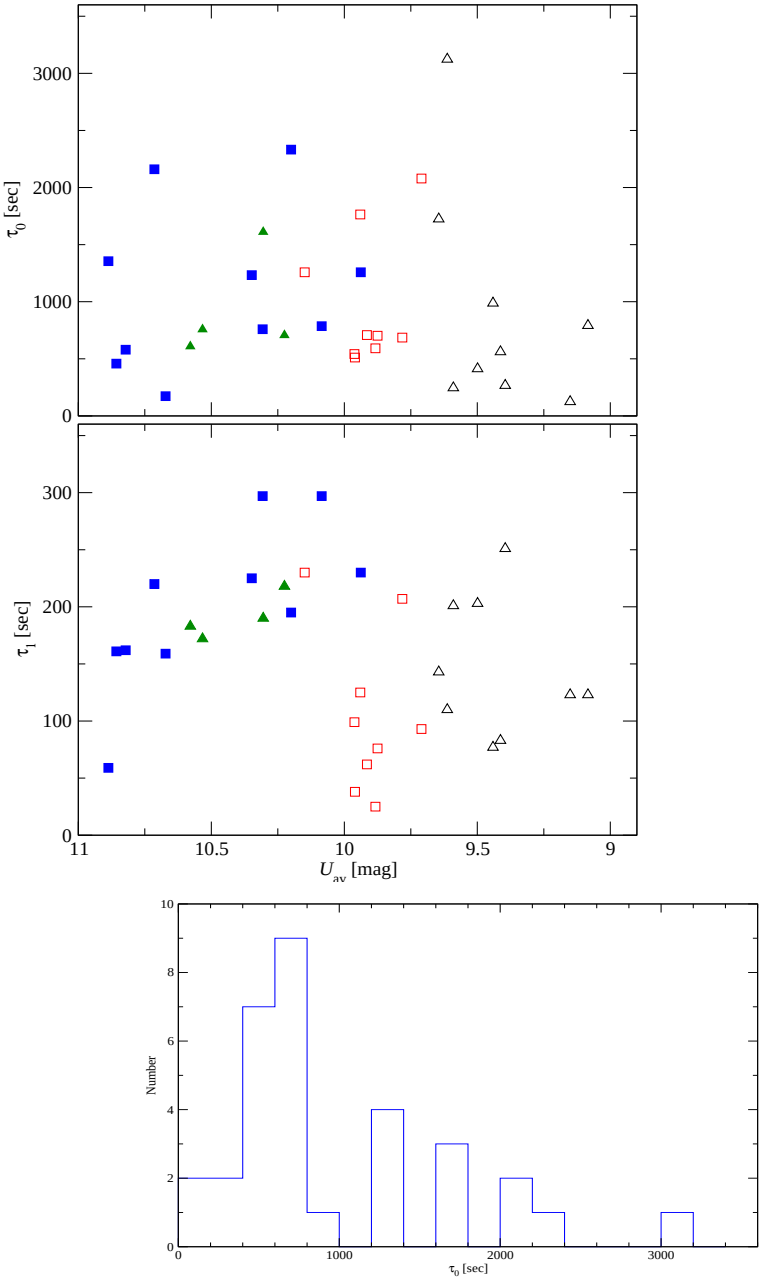

Fig. 5. Relation between the e-folding time of the ACF for lower frequency variability τ_0 (top) and for higher frequency variability τ_1 (bottom) versus U magnitude. The symbols are the same as in Fig.2. The four shortest e-folding times τ_0 are practically the same as the corresponding e-folding times τ_1 obtained from these series. Histogram showing the distribution of the e-folding times τ_0. The four shortest values are practically the same as corresponding e-folding times τ_1 obtained during the same night.

$\overline{\sigma}_1 \approx 0.04 \pm 0.01$; however some points during the second observational season (December 1990 – March 1991) are close to the detection level of about 0.010-0.015 magnitude.

4.3 Inner disk radius

The source of flickering in symbiotic binaries can be associated with the white dwarf surface, its magnetosphere or the inner parts of an accretion disc.

Sokoloski & Kenyon (2003a) argued that the time scale of the smooth variations can represent the dynamical (Keplerian) time at the inner edge of a truncated disk (or a disk in which emission is truncated).

In this case we can estimate the inner disk radius:

$$R_{in} \sim (2\pi)^{-2/3} G^{1/3} (t_{dyn})^{2/3} M_{wd}^{1/3} \quad (2)$$

The typical time scale of the smooth variations in MWC 560 is $\sim$1 hour, as is visible on Fig.3. The shorter time variations observed in MWC 560 have typical time scales of 10-15 minutes. For a 1.2 $M_\odot$ WD this will correspond to an inner disk radius $R_{in} \sim 1.3 R_\odot$ for t_{dyn} $\sim$1 hour, and $R_{in} \sim 0.4 R_\odot$ for t_{dyn} $\sim$10 min.

Because $R_{in} >> R_{ej}$ perhaps there is a non-emitting part in the disk in between R_{ej} and R_{in} or exactly this part supplies the material for the outflow.

4.4 Disk-jet connection

From the above considerations (supposing that the accretion is indeed via an accretion disk) the following picture emerges:

(1) the innermost disk is disrupted (or non-emitting) during the whole period of the observations, because we do not see large flickering variability on time scales shorter than 10-15 min, like those in T CrB on time scales $\leq$5 min (see Sect.3).

(2) During the period of discrete jet ejections with variable velocities (January 1990 - April 1990), there are smooth variations on time scales of $\sim$1 hour, which indicate an inner disk radius $R_{in} \sim 1.3 R_\odot$.

(3) During December 1990 - March 1991 the outflow is stable with V_{ej} $\approx$900 km s^{-1}, the amplitude of the variability is sometimes very low, and no characteristic time can be defined. This probably indicates that $R_{in} > 1.5 R_\odot$.

(4) During September 1991 - March 1993 stable outflow with V_{ej} $\sim$2000 km s^{-1} is accompanied by variations on time scales from 10 min to 1 hour, which indicate $R_{in} \sim 0.4 R_\odot$.

The presence of only smooth variations on time scales of $\sim$1 hour is similar to the observed behaviour of CH Cyg in April and June 1997 (Sokoloski & Kenyon 2003a) when the star produced a radio jet (Karovska et al. 1998). The light curves of MWC 560 from September 1991 - March 1993 are somewhat similar to those observed in CH Cyg in August 1997 (Sokoloski & Kenyon 2003b).

MWC 560 never (at least in the present data set) has displayed large amplitude flickering on time scales $\sim$5 min like that observed usually in CH Cyg and cataclysmic variables (i.e. light curves of CH Cyg in July and August 1998 from Sokoloski & Kenyon 2003b). This indicates that during 1990-1993 the inner part the disk of MWC 560 had never been built up entirely or it is always non-emitting.

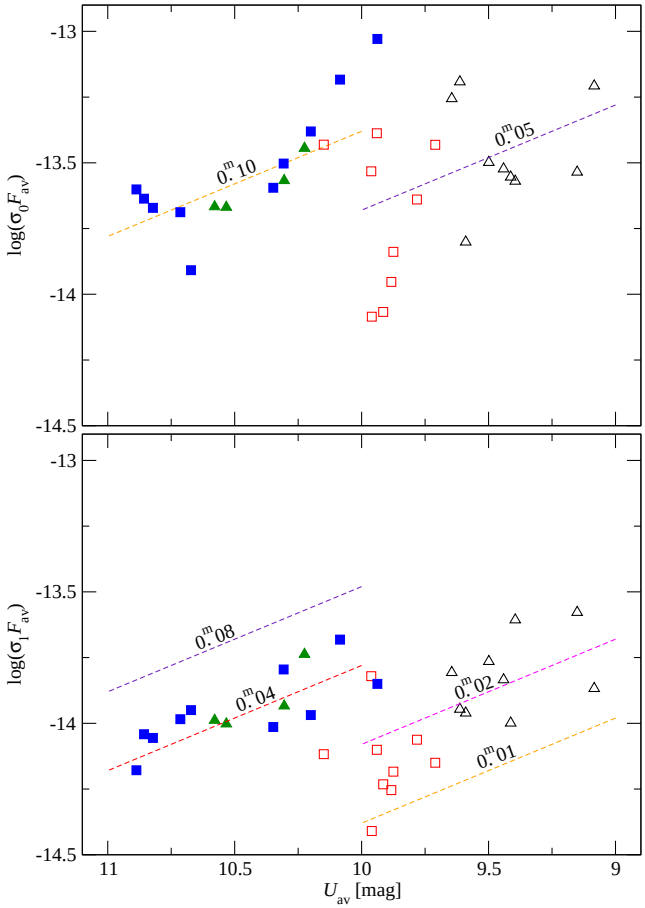

Fig. 6. Relation between values of σ_0 (top) and σ_1 (bottom) in flux units [ergs s^{-1} cm^{-2} A^{-1}] for lower and higher frequencies, respectively versus U magnitude. The symbols are the same as in Fig.2. The lines show relations for constant values of σ_0 and σ_1 in magnitudes. The detection level is about 0.01 magnitude.

It seems that the central region of the accretion disk is able to switch between different states. In the Galactic microquasar GRS 1915+105 Belloni et al. (1997, 2000) interpret the transition between different states as being caused by the disappearance and reappearance of the inner accretion disk. It seems that MWC 560 and CH Cyg also display a more or less similar behaviour.

Possible physical mechanisms can be (i) a magnetic switch which results in variation of the jet speeds as discussed by Meier et al. (1997), (ii) a disk instability mechanism of the kind thought to occur in dwarf novae and other cataclysmic variables.

5 Conclusions

We have analyzed archival data of the flickering in U band of the jet-ejecting symbiotic star MWC 560 obtained during the time interval 1990-1993. We have shown that there is a connection in MWC 560 between the mass outflow state (jets) and the properties of the flickering.

(1) The short term variability (on time scales $<$20 min) is missing during the period February 1990 – March 1991, when the mass outflow is in a regime of discrete ejections with V_{ej} up to 7000 km s^{-1}, and when the outflow has a stable V_{ej} $\sim$900 km s^{-1}.

(2) A short term variability on time scales of 10-15 minutes is apparent during December 1991 – January 1993, when the outflow has a more or less stable velocity $\sim$2000 km s^{-1}.

(3) The flickering amplitude is influenced by the different states of the jet (the lowest values of the amplitude correspond to the state with V_{ej} $\sim$900 km s^{-1}). This is probably the reason why no correlation like those observed in T CrB and CH Cyg is visible.

(4) The power spectra of MWC 560 follow roughly a power law with $\overline{\gamma} = -0.95 \pm 0.22$. The e-folding time of the ACF exhibits bigger scatter, if we compare it with the "stable disk" of T CrB. A comparison with T CrB shows also that the variability of MWC 560 on time scales $\leq 5 - 10$ min is considerably lower.

The most probable interpretation of these results is that the inner part of the accretion disk switches between different states. The observed disk-jet connection in this binary system seems to be similar to that observed in CH Cyg and some microquasars. The observational evidence for a disk-jet connection in MWC 560 and CH Cyg in addition to the other similarities (see also Zamanov & Marziani 2002) supports the idea that these objects represent very good non-relativistic analogs of black hole accretors.

More observations in different states are necessary to define better the properties of the accretion process and how it is connected with the mass outflow regimes. Especially useful will be if the spectra and the photometry runs are obtained simultaneously or in the same night.

Acknowledgments

This research has made use of SIMBAD, IRAF, MIDAS and Starlink and was partially supported by Bulgarian NSF (HTC01-152).

References

Belczyński, K., Mikołajewska, J., Munari, U., Ivison, R. J., & Friedjung, M.: 2000, A&AS 146, 407
Belloni, T., Mendez, M., King, A. R., van der Klis, M., & van Paradijs, J. 1997, ApJ, 488, L109
Belloni, T., Klein-Wolt, M., Méndez, M., van der Klis, M., & van Paradijs, J. 2000, A&A, 355, 271
Bessell, M. S. 1979, PASP, 91, 589
Brocksopp, C., Fender, R. P., Larionov, V., Lyuty, V. M., Tarasov, A. E., Pooley, G. G., Paciesas, W. S., & Roche, P. 1999, MNRAS, 309, 1063
Bruch, A. & Duschl, W. J. 1993, A&A, 275, 219
Bruch, A. 1992, A&A 266, 237
Bruch, A. 2000, A&A , 359, 998
Choudhury, M., Rao, A. R., Vadawale, S. V., Ishwara-Chandra, C. H., & Jain, A. K. 2002, A&A, 383, L35
Corbel, S., Fender, R. P., Tzioumis, A. K., Nowak, M., McIntyre, V., Durouchoux, P., & Sood, R. 2000, A&A, 359, 251
Dobrzycka, D., Kenyon, S. J., & Milone, A. A. E. 1996, AJ, 111, 414
Fluks, M. A., Plez, B., The, P. S., de Winter, D., Westerlund, B. E., & Steenman, H. C. 1994, A&AS, 105, 311
Gromadzki, M., Mikołajewska, J., Whitelock, P. A., & Marang, F. 2007, A&A, 463, 703
Iijima, T. 2002, A&A, 391, 617
Karovska, M., Carilli, C. L., & Mattei, J. A. 1998, The Journal of the American Association of Variale Star Observers, vol. 26, no. 2, p. 97-100
Kraicheva, Z., Stanishev, V., Genkov, V., & Iliev, L., 1999, A&A, 351, 607
Lee, T. A. 1970, ApJ, 162, 217
Livio, M. 1997, IAU Colloq. 163: Accretion Phenomena and Related Outflows, 121, p. 845
Livio, M. 1998, Wild Stars In The Old West: Proceedings of the 13th North American Workshop on Cataclysmic Variables and Related Objects, ASP Conference Series, Vol. 137, 1998, ed. S. Howell, E. Kuulkers, and C. Woodward (1998), p.264
Livio, M., Pringle, J. E., & King, A. R. 2003, ApJ, 593, 184
Madej, J., Należyty, M., & Althaus, L. G., 2004, A&A, 419, L5
Meier, D. L., Edgington, S., Godon, P., Payne, D. G., & Lind, K. R., 1997, Nature, 388, 350
Mirabel, I. F. & Rodriguez, L. F. 1998, Nature, 392, 673
Michalitsianos, A. G., Perez, M., Shore, S. N., et al., 1993, ApJ, 409, L53
Mikolajewski, M., Mikolajewska, J., Tomov, T., Kulesza, B., Szczerba, R. 1990, Acta Astronomica, 40, 129
Panek, R. J., 1980, ApJ, 241, 1077
Robinson, E. L. & Nather, R. E., 1979, ApJS, 39, 461
Schmidt-Kaler, T. H. 1982, in Landolt-Boernstein, New Series, Group VI, Vol. 2b, Stars and Star Clusters, ed. K. Schaifers & H. H. Voigt (New York: Springer), p. 14
Schmid, H. M., Kaufer, A., Camenzind, M., Rivinius, T., Stahl, O., Szeifert, T., Tubbesing, S., & Wolf, B. 2001, A&A, 377, 206
Shore, S. N., Aufdenberg, J. P., & Michalitsianos, A. G., 1994, AJ, 108, 671
Sokoloski, J. L. & Kenyon, S. J. 2003a, ApJ 584, 1021
Sokoloski, J. L. & Kenyon, S. J. 2003b, ApJ 584, 1027
Sokoloski, J. L., Bildsten, L., & Ho, W. C. G. 2001, MNRAS, 326, 553
Suh, I.-S., & Mathews, G. J. 2000, ApJ 530, 949
Tomov, T., Kolev, D., Zamanov, R., Georgiev, L., & Antov, A. 1990, Nature, 346, 637
Tomov, T., Kolev D., Ivanov M., Antov A., Jones A., Mikołajewski M., Lepardo A., et al. 1996, A&AS 116, 1
Tomov, T., Zamanov, R., Kolev, D., Georgiev, L., Antov, A., Mikolajewski, M., & Esipov, V. 1992, MNRAS 258, 23
Tomov, T. & Kolev, D. 1997, A&AS, 122, 43
Warner, B. 1995, Cataclysmic variable stars, Cambridge Astrophysics Series, Cambridge, New York: Cambridge University Press
Yonehara, A., Mineshige, S., & Welsh, W. F. 1997, ApJ 486, 388
Zamanov, R. K. & Bruch, A. 1998, A&A, 338, 988
Zamanov, R. & Marziani, P. 2002, ApJ, 571, L77
Zamanov, R., Bode, M. F., Stanishev, V., & Martí, J. 2004, MNRAS, 350, 1477
Zamanov, R. K., Gomboc, A., Stoyanov, K. A., & Stateva, I. K. 2010, Astronomische Nachrichten, 331, 282